Atmos. Chem. Phys. Discuss., 11, 31475–31493, 2011
www.atmos-chem-phys-discuss.net/11/31475/2011/
doi:10.5194/acpd-11-31475-2011

Atmospheric Chemistry and Physics Discussions

Vertical mixing in the lower troposphere by mountain waves over Arctic Scandinavia

M. Mihalikova[1,2] **and S. Kirkwood**[1,2]

[1]Polar Atmospheric Research, Swedish Institute of Space Physics, Box 812, 98128, Kiruna, Sweden
[2]Dept. of Space Technology, Luleå Technical University, Kiruna, Sweden

Received: 4 November 2011 – Accepted: 12 November 2011 – Published: 1 December 2011

Correspondence to: M. Mihalikova (maria.mihalikova@irf.se)

Published by Copernicus Publications on behalf of the European Geosciences Union.

Abstract

Measurements made by ozonesondes and by a 52 MHz wind-profiling radar during February and March 1997 are studied. The radar is located at Esrange, near Kiruna in Arctic Sweden, on the eastern flank of the Scandinavian mountains. Daily ozonesondes were launched from the same site. The radar vertical and horizontal wind measurements are used to identify times when mountain waves were present. Mean vertical gradients in ozone mixing ratio in the lower troposphere are determined in conditions with mountain waves present and when they were absent. Back-trajectories were calculated so that only air-masses with their origin to the west of the mountains were included in the final averages. The vertical gradient in ozone mixing ratio is found to be about twice as steep outside wave conditions as it is during mountain waves. This suggests a very high rate of vertical mixing, with an average eddy diffusivity of order 5000 $m^2 s^{-1}$. This is consistent with an earlier estimate of the occurrence rate of complete mixing by wave breaking over the mountain range.

1 Introduction

The air circulation over Scandinavia is, similarly to the rest of Europe, largely influenced by the Icelandic low, which is one of the principal centres of action in the general circulation of the Northern Hemisphere and is most pronounced in winter months. As a result, the prevailing airflow over Scandinavia is from western directions. The Scandinavian range is perpendicular or nearly perpendicular to these wind directions thus creating a significant barrier for the winds. Consequently, this can often lead to the formation of mountain lee waves and turbulence associated with those waves. This turbulence can be readily observed with the ESRAD (ESrange RADar) VHF wind-profiling radar, which is situated on the lee side of Scandinavian mountain range (see e.g., Satheesan and Kirkwood, 2010). Turbulence associated with breaking of mountain waves has been recognized as a potential source of vertical mixing of atmospheric constituents

ACPD
11, 31475–31493, 2011

(Kirkwood et al., 2010, and references therein). However, its significance in quantitative terms needs still to be determined. We here try to look at this in terms of vertical down-mixing of ozone. Ozone is transported from the stratosphere to the troposphere through several mechanisms, one of them being tropopause folds, which can bring stratospheric air to low altitudes (Shapiro, 1980; Rao and Kirkwood, 2005; Hocking et al., 2007). There is significant seasonal variation in tropopause folds over Northern Scandinavia, with a winter maximum in their occurrence (Rao et al., 2008). They are most of the time related with strong westerly winds, which are a precursor for the creation of mountain lee waves and also create potential for formation of associated turbulence (Rao and Kirkwood, 2005).

Radar observations help to qualitatively assess the occurrence of turbulent mixing in the lower troposphere. However, quantitative estimates of vertical mixing and of eddy diffusion rates, in turbulence associated with mountain waves, are very sensitive to the value of buoyancy frequency (ω_B), There is large uncertainty in this parameter within the narrow layers where the turbulent mixing most probably occurs (Kirkwood et al., 2010). Better understanding and quantitative estimates of these processes, in connection with the maximum occurrence of tropopause folds in winter time, might help to explain the unexplained seasonal variation in surface ozone in the polar regions, with observed higher wintertime concentrations than those predicted by models (Tarasova et al., 2007). An idea about the behaviour of ozone profiles in these situations can be gained by further investigating winter tropospheric ozone profiles during and outside periods of mountain-wave activity.

2 Data and analysis

2.1 Ozonesondes

Radio and ozone sonde measurements from ESRANGE-Kiruna (67.9° N, 21.1° E) made between 1 February 1997 and 25 March 1997 as part of the ILAS (Improved

ACPD
11, 31475–31493, 2011

Limb Atmospheric Spectrometer) validation balloon campaign (Kreher et al., 1999) have been used. Ozone and temperature profile measurements were made almost every day. 57 ECC (Electrochemical Concentration Cell) balloon-borne ozonesondes interfaced with Vaisala RS80 meteorological radiosondes were used. Measurements of ozone partial pressure (mPa), air pressure (hPa), air temperature (°C), humidity (%) and ozone pump temperature (°C) were recorded around each 10 s which resulted in 30–60 m vertical resolution (Kreher et al., 1999). Profiles were visually examined at heights up to 10 km and erroneous data was excluded based on sudden discontinuation of data and extremely unusual values of data. The accuracy of ozone partial pressure measurements of ECC sondes in the troposphere and lower stratosphere is typically ± 5 % (Kreher et al., 1999). In this same time period we also initially considered ozone sondes from other sites (Sodankyla, Ny Ålesund, Lerwick and Scoresbysund) from both sides of the Scandinavian mountain range, although the measurements from these sites were not as frequent. By investigating these sets of data we hoped to make a first estimate of the importance of mountain-wave induced mixing.

After dividing the profiles into groups according to the presence or absence of mountain waves (see Sect. 2.2), mean profiles of ozone mixing ratio, potential temperature, pressure and height were calculated for each group. Let us for convenience from now on refer to the profiles as "in-wave profile" – for the group when mountain waves were observed and "outside-wave profile" – for the second group. Mean profiles were calculated by assigning mean values of ozone, temperature, pressure and height to layers of 100 m thickness, and the initial result for sondes launched from Esrange is shown in Fig. 1.

2.2 ESRAD MST radar

ESRAD is interferometric VHF wind-profiling radar, located at Esrange in Northern Sweden (67.54° N, 21.04° E) at an altitude of 295 m a.s.l. It operates at a frequency of 52 MHz and has been operating nearly continuously since August 1996. (Chilson et al., 1999) ESRAD characteristics during winter 1996/1997 are shown in Table 1.

ACPD
11, 31475–31493, 2011

To divide the profiles into groups based on the presence or absence of mountain waves, measurements by ESRAD around the height of 3 km were used. At this height we can see the signature of air movements in the mountain waves in ESRAD data. ESRAD is operated with a vertically pointing beam and determines the horizontal wind movements with the help of full-correlation analysis. This method assumes that scatterers are moving with the mean wind and determines the wind movements based on the movement of the diffraction pattern received in the radar's 6 separate receivers. The vertical scatterer drift is computed from the doppler shift of the returned signal. In cases of mountain waves we can see a pattern of upwards and downwards air movements, varying through the time of measurement. To distinguish the mountain wave periods, and ensure accurate wind measurements, a set of conditions were applied to the data. The signal to noise ratio had to be bigger than a factor 2 (to exclude uncertain data), the wind speed perpendicular to the mountain range had to be finite and not zero, and the absolute value of vertical speed had to be greater than 0.2 m s^{-1}. If these conditions were met within 3 h before or after an ozonesonde launch, the sonde would be considered as belonging to the group with mountain waves present. The difference between the two groups of data can also be illustrated by calculating the root mean square of vertical velocity (V_{RMS}) within each 1 min sampling interval (from the correlation time of the echoes). This quantifies the vertical velocity fluctuations which are a characteristic of turbulence kinetic energy. We have calculated that, in this dataset, the root mean square of vertical velocity in wave conditions (0.25 m s^{-1}) is about 40 % higher than outside wave conditions (0.18 m s^{-1}) at 3 km height.

2.3 Trajectory tracing

To investigate the sources of air masses arriving at Esrange, for each ozonesonde, back-trajectories were calculated from the launch time using the Flexpart model (Stohl et al., 2005). ECMWF (European Centre for Medium Range Weather Forecasts) data were used as model input. The 4 d back-trajectories were calculated for 1, 2, 3, 4 and 5 km heights for each sonde launch. Initially we attempted, with help of these back-trajectories, to find a connection between ozonesondes launched at Esrange and the ozonesondes available from other stations (Sodankyla, Ny Ålesund, Lerwick and Scoresbysund). This was done by examining the distance of the back-trajectories from those stations and the time the air masses at various levels were passing by the stations. As the sonde measurements were not part of a coordinated experiment, we did not manage to positively link any two of them with high enough confidence. Also, with prolonged daylight in late February and March, photo-chemistry could potentially affect ozone on the longer distances involved.

Instead, we have concentrated on the difference in back-trajectories between the investigated groups, using only the sondes from Esrange. As we can see in Fig. 1a) there is a nearly constant difference of 4 K between the mean profiles of potential temperature between outside-wave and in-wave profiles. That was the main reason for us to compare the sources of air masses (Fig. 2). As we can see, the sources of air masses for all heights in the outside-waves group are more evenly distributed both to the west and to the east from Esrange (Atlantic Ocean and Continental Asia) suggesting bigger variation in the original amounts of ozone in the air masses and thus a possible reason for difference in the profiles. The sources for the in-wave group lie predominantly to the west from Esrange mainly in the area between the British Isles, Iceland, and the east coast of Canada. This difference in the location of sources of air masses was to be expected because of the conditions that need to be satisfied for creation of mountain waves. The air needs to come to Esrange from directions close to perpendicular to Scandinavian mountain range which would be southwest to northwest directions. Air arriving from these directions comes most of the times from the rear side of the Icelandic low, which is a quasi-permanent centre of action in the general air circulation of the Northern Hemisphere and is more pronounced in winter times. This is in agreement with the positions of sources in our figure. To try to minimise the contribution of the difference in the air mass sources to the mean profiles, we have decided to investigate more closely only cases when the air masses arrived at Esrange from western directions. Based on the back-trajectories we have chosen only sondes where back-

ACPD
11, 31475–31493, 2011

trajectories at all heights had sources lying to the west from Esrange (Fig. 3). This selection cut down the number of ozonesondes from the initial 54 to only 23, of which only 6 arrived outside of wave conditions. The mean profiles using this restricted set of sondes are shown in Fig. 4.

3 Results

The mean profiles of ozone in the presence of mountain waves and outside of mountain wave conditions, using all available sondes, are compared in Fig. 1. When looking at the height profiles of ozone mixing ratio, we can see that, in the lower heights (600 to around 2000 m) the gradient of ozone mixing ratio for the in-wave profile is similar to the outside-wave profile (3.3 ppb km^{-1} for outside-wave profile and 3.5 ppb km^{-1} for in-wave profile) but the values in individual layers differ with the in-wave profile having ozone mixing ratio values 2.5 to 3 ppb higher up to around 2000 m. Above this layer, we can recognize a height region from 2000 m to around 3600 m where the gradient of ozone mixing ratio in the outside-wave profile (5.1 ppb km^{-1}) grows to be more than two times as high as the gradient for the in-wave profile (1.9 ppb km^{-1}). Because of this difference in gradients, the outside-wave profile overtakes the wave profile around 2500 m height and grows to be some 2.5 ppb higher in 3600 m. Above this height the gradients in the tropospheric parts of the profiles become virtually the same, with the in-wave profile soon catching up in values and both profiles having similar values up to the maximum height considered here 6000 m. What interests us most is the difference in the profiles up to 3600 m that was made visible in our mean profiles and which would suggest that, during times of mountain waves and associated turbulence, the ozone in this layer is mixed better and its downward flux is higher. However, we can see from the potential temperature profiles that there is systematic offset between in-wave and outside-wave profiles of potential temperature by up to 4 K. This is one of the reasons why we have decided to investigate more closely the sources of the arriving air masses. After choosing only sondes with similar origins of air masses (to the

ACPD
11, 31475–31493, 2011

west of Scandinavia) as described in the previous section, the same comparison can be made using this new subset of sondes. The mean ozone mixing ratio and potential temperature profiles are compared in Fig. 4. In the potential temperature profile, we can see that the difference of around 4 K between the profiles was eliminated, but we still can observe a difference in the gradient of potential temperature from the ground up to 4000 m. The in-wave profile has a more constant gradient in the whole layer with values of potential temperature higher than the outside-wave profile in the lower part (up to around 1500 m) and then lower values up to 4000 m where the gradients and values of potential temperature for both profiles become similar. This can be a sign of turbulent mixing in the in-wave layer. When looking at the mean ozone mixing ratio profile we discover similar features as in Fig. 1. In the layer from 600 m to around 1100 m, the in-wave profile shows around 4 ppb higher values of ozone mixing ratio. Above this layer the ozone mixing ratio for outside-wave profile rises two times as quickly as for the in-wave profile, up to the height 3600 m. In this layer the outside-wave profile has a gradient 5.2 ppb km^{-1} and in-wave profile has a gradient 2.2 ppb km^{-1}. Above the height 3600 m, again the values of ozone mixing ratios as well as gradients become similar in both profiles. When analysing individual profiles in these groups (not shown), we can see that, in the outside-wave group, temperature inversions are present in various layers at heights up to 2000 m in all of the 6 profiles of this group. Stable stratifications of these layers prohibits development of extensive vertical mixing of atmospheric constituents like ozone. Above 2000 m we can observe a faster rise in the ozone mixing ratios. There are temperature inversions at heights up to 2000 m present also under in-wave conditions, although they are generally shallower structures, and present in less than half of the 17 profiles of the in-wave group.

4 Discussion

We have presented in-wave and outside-wave mean profiles of ozone which were constructed based on a set of ozonesondes launched at Esrange during the ILAS

ACPD
11, 31475–31493, 2011

validationh campaign in February and March 1997, and have divided them into in-wave and outside-wave groups with the help of ESRAD radar data. The main difference is in the behaviour of the profiles in the lower troposphere, where the difference in gradient is evident and the in-wave profile values of mixing ratio reach 4 ppb higher values than the values in outside-wave profile. At the same time, from the analysed set of sondes, we did not observe any significant difference between the column densities of ozone in the lower troposphere (heights 600 m to 3600 m). The amount of ozone in a column of air in the outside-wave profile was 10.37 DU and only a slightly higher value in the wave profile 10.43 DU. This similarly, in addition to the potential temperature values, supports the view that the sources are air masses with similar properties.

After excluding erroneous data and choosing only sondes with similar point of origin of the air masses, we were able to use only 23 sondes of which 6 were measured under the outside-wave conditions and 17 under in-wave conditions. Since we have attempted a statistical look at the data, the low number of observations may influence our result. To ensure a more representative result, we have decided to concentrate on ozone profiles under the height of the lowest identified tropopause fold to avoid any influence of high values of ozone in the fold structures on the gradient of ozone mixing ratio. This way we hope to represent better the behaviour of ozone profiles in the turbulent areas. By choosing only the sondes with similar sources of air masses, arriving at Esrange from western directions, we have constructed mean profiles that could be considered to have similar sources on the western side of the Scandinavian mountain range. The only difference between them when they arrive at Esrange would be in the time that the air masses of the in-wave group have spent time in an area influenced by mountain waves and associated turbulence. The length of the path affected by this turbulence is around 100 km (Kirkwood et al., 2010). Over this distance, in winter months, we can also regard the effect of chemistry on ozone in the troposphere to be insignificant. Hence, we can consider the differences in the mean profiles of ozone concentration and potential temperature to be caused primarily by the mixing occurring under the turbulent conditions. We can use the characteristic time for vertical mixing

ACPD
11, 31475–31493, 2011

(relaxation of the vertical gradient of ozone mixing ratio), which is given by (Goody, 1995):

$$\tau_K \sim \frac{H^2}{K}, \tag{1}$$

to estimate the eddy diffusion coefficient K. H is the density scale height (over which the mixing ratio varies significantly) and is ~7 km. Since the vertical gradient of ozone mixing ratio is about halved between the in-wave and outside-wave profiles, τ_K in this interpretation corresponds to the time that the air mass spend in the turbulent region while crossing the Scandinavian mountain range. From ESRAD measurements we find that the mean wind speeds perpendicular to the mountain range at the height of 3 km, was 10.9 m s^{-1} in wave conditions. The characteristic time for vertical mixing in our case can be estimated to be 100 km divided by this speed, i.e. ~2.5 h. Consequently the eddy diffusion coefficient $K \sim 5000\,\mathrm{m^2\,s^{-1}}$. This is a very high value, for example 1–2 orders of magnitude higher than values estimated for the extreme conditions of a hurricane (Zhang et al., 2011), and in the Arctic lower troposphere vertical mixing is generally assumed to be negligible ($K \sim 0$) because of the high average static stability (e.g., Barrie and Platt, 1997). However, the possibility of complete mixing in mountain lee waves is well recognised (Durran, 2003). According to the 3-D simulations of mixing by breaking gravity waves by Fritts et al. (2003), the time for mixing in such conditions is less than the buoyancy period (a few minutes). Applying Eq. (1) with $\tau_K = 600$ s gives $K \sim 10^5\,\mathrm{m^2\,s^{-1}}$. The study by Kirkwood et al. (2010) showed that the probability that an air-mass between 1000 m and 5000 m height will encounter a region of wave breaking during its passage across the mountains could be as high as 5–10 %. This would imply average values of $K \sim 5000$–$10\,000\,\mathrm{m^2\,s^{-1}}$, consistent with our estimate here based on the ozone mixing ratio gradient.

It should be pointed out that our estimate of $K \sim 5000\,\mathrm{m^2\,s^{-1}}$ is 3 orders of magnitude larger than the value that can be found using the usual method of estimating eddy diffusivity from radar and sonde observations, where K is given as (see e.g., Wilson,

Discussion Paper | Discussion Paper | Discussion Paper | Discussion Paper |

ACPD
11, 31475–31493, 2011

Vertical mixing by mountain waves

M. Mihalikova and S. Kirkwood

2004):

$$K \sim \frac{V_{\mathrm{RMS}}^2}{\omega_{\mathrm{B}}}. \tag{2}$$

From our radar measurements we have the value of V_{RMS} in wave conditions $0.25\,\mathrm{m\,s^{-1}}$ and we have calculated buoyancy frequency ω_{B} in the lower troposphere from the mean sonde profiles to be $\sim 1.1 \times 10^{-2}\,\mathrm{s^{-1}}$. Then the eddy diffusion coefficient $K = \sim 2.3\,\mathrm{m^2\,s^{-1}}$ and the characteristic time of vertical mixing according to Eq. (1) through the scale height would be approximately 247 days. However, as we can see in Eq. (2), eddy diffusion coefficient is very sensitive to the value of ω_{B}. As discussed in Kirkwood et al. (2010), the mean value of ω_{B} may not be representative, especially when turbulence occurs in thin layers where ω_{B} drops close to zero values. Given the fine structure of the profile of ω_{B} over the troposphere, estimates based on average radar V_{RMS} in combination with low resolution estimates of ω_{B}, are not adequate for calculation of vertical mixing characteristics in mountain-wave conditions.

The difference of 4 ppb ($7.9\,\mathrm{\mu g\,m^{-3}}$ at measured mean temperature and pressure) between in-wave and outside-wave conditions which we find in the lower levels of troposphere is of the same order as typical diurnal variations of ground ozone. The mean amplitude of variations of ozone within each day in February and March 1997 is, according to ground ozone measurements performed in Esrange, $9.8\,\mathrm{\mu g\,m^{-3}}$ (based on hourly means of ozone concentrations, http://www.ivl.se/tjanster/datavardskap/luftkvalitet.html). From this we can conclude that in individual cases the changes in ground ozone concentrations can be highly influenced by turbulent downmixing of ozone from higher altitudes. As has been previously shown (Terao et al., 2008) the seasonal ozone changes in the middle troposphere can be linked and are correlated with the changes of ozone in lower stratosphere. This stratosphere-troposphere exchange is driven by synoptic scale processes e.g. tropopause folds. In the presence of mountain waves during these events, ozone is more efficiently downmixed and can influence the levels of ground ozone.

Another source of uncertainty is the role of tropospheric ozone photochemistry. We have chosen to analyse measurements during winter time when the ozone lifetime is long to minimise the influence of tropospheric photochemistry on our results. However, there are still uncertainties in the rates of deposition of ozone into the snow-covered landscapes (Helmig et al., 2007). The uncertainty in ozone surface fluxes constitutes an uncertainty in the importance of downmixed ozone on ground ozone concentrations. For better understanding and for better determination of the influence of turbulence in mountain wave conditions on the concentrations of ozone in lower troposphere and ground level ozone, more measurements are needed of ozone profiles in targeted conditions, preferably including observations in air masses crossing the Scandinavian mountain range from both sides of the range.

Acknowledgements. We greatfully acknowledge support for this research from Swedish Research Council. M. Mihalikova is supported by the Swedish National Graduate School of Space Technology, Luleå University of Technology. The ozone sonde data were provided by Improved Limb Atmospheric Spectrometer validation balloon campaign.

References

Barrie, L. and Platt, U.: Arctic tropospheric chemistry: an overview, Tellus B, 49, 450–454, doi:10.1034/j.1600-0889.49.issue5.2.x, 1997. 31484

Chilson, P., Kirkwood, S., and Nilsson, A.: The Esrange MST radar: a brief introduction and procedure for range validation using balloons, Radio Sci., 34, 427–436, 1999. 31478

Durran, D.: Lee waves and mountain waves, in: Encyclopedia of Atmospheric Sciences, edited by in Chief: Holton, J. R., Academic Press, Oxford, 1161 – 1169, doi:10.1016/B0-12-227090-8/00202-5, 2003. 31484

Fritts, D. C., Bizon, C., Werne, J. A., and Meyer, C. K.: Layering accompanying turbulence generation due to shear instability and gravity wave breaking, J. Geophys. Res., 108, doi:10.1029/2002JD002406, 2003. 31484

Goody, R.: Principles of atmospheric physics and chemistry, Oxford University Press, http://books.google.com/books?id=_vzPJz2XUfcC, New York, ISBN:0-19-509362-3, 1995. 31484

Helmig, D., Ganzeveld, L., Butler, T., and Oltmans, S. J.: The role of ozone atmosphere-snow gas exchange on polar, boundary-layer tropospheric ozone – a review and sensitivity analysis, Atmos. Chem. Phys., 7, 15–30, doi:10.5194/acp-7-15-2007, 2007. 31486

Hocking, W., Carey-Smith, T., Tarasick, D. W., Argall, P. S., Strong, K., Rochon, Y., Zawadzki, I., and Taylor, P. A.: Detection of stratospheric ozone intrusions by windprofiler radars, Nature, 450, 281–284, doi:doi:10.1038/nature06312, 2007. 31477

Kirkwood, S., Mihalikova, M., Rao, T. N., and Satheesan, K.: Turbulence associated with mountain waves over Northern Scandinavia – a case study using the ESRAD VHF radar and the WRF mesoscale model, Atmos. Chem. Phys., 10, 3583–3599, doi:10.5194/acp-10-3583-2010, 2010. 31477, 31483, 31484, 31485

Kreher, K., Bodeker, G. E., Kanzawa, H., Nakane, H., and Sasano, Y.: Ozone and temperature profiles measured above Kiruna inside, at the edge of, and outside the Arctic Polar Vortex in February and March 1997, Geophys. Res. Lett., 26, 715–718, 1999. 31478

Rao, T. N. and Kirkwood, S.: Characteristics of tropopause folds over Arctic latitudes, J. Geophys. Res., 110, doi:10.1029/2004JD005374, 2005. 31477

Rao, T. N., Arvelius, J., and Kirkwood, S.: Climatology of tropopause folds over a European Arctic station (Esrange), J. Geophys. Res., 113, doi:10.1029/2007JD009638, 2008. 31477

Satheesan, K. and Kirkwood, S.: Turbulence for different background conditions using fuzzy logic and clustering, Ann. Geophys., 28, 1475–1481, doi:10.5194/angeo-28-1475-2010, 2010. 31476

Shapiro, M. A.: Turbulent mixing within tropopause folds as a mechanism for the exchange of chemical constituents between the stratosphere and troposphere, J. Atmos. Sci., 37, 994–1004, doi:10.1175/1520-0469(1980)037¡0994:TMWTFA¿2.0.CO;2, 1980. 31477

Stohl, A., Forster, C., Frank, A., Seibert, P., and Wotawa, G.: Technical note: The Lagrangian particle dispersion model FLEXPART version 6.2, Atmos. Chem. Phys., 5, 2461–2474, doi:10.5194/acp-5-2461-2005, 2005. 31479

Tarasova, O. A., Brenninkmeijer, C. A. M., Jöckel, P., Zvyagintsev, A. M., and Kuznetsov, G. I.: A climatology of surface ozone in the extra tropics: cluster analysis of observations and model results, Atmos. Chem. Phys., 7, 6099–6117, doi:10.5194/acp-7-6099-2007, 2007. 31477

Terao, Y., Logan, J. A., Douglass, A. R., and Stolarski, R. S.: Contribution of stratospheric ozone

to the interannual variability of tropospheric ozone in the northern extratropics, J. Geophys. Res., 113, doi:10.1029/2008JD009854, 2008. 31485
Wilson, R.: Turbulent diffusivity in the free atmosphere inferred from MST radar measurements: a review, Ann. Geophys., 22, 3869–3887, doi:10.5194/angeo-22-3869-2004, 2004. 31484
Zhang, J. A., Marks, F. D., Montgomery, M. T., and Lorsolo, S.: An estimation of turbulent characteristics in the low-level region of intense hurricanes Allen (1980) and Hugo (1989), Mon. Weather Rev., 139, 1447–1462, doi:10.1175/2010MWR3435.1, 2011. 31484

ACPD
11, 31475–31493, 2011

Table 1. ESRAD characteristics during winter 1996/1997 for the measurement mode used in this study.

Location	67.54° N, 21.04° E
Altitude	295 m a.s.l.
Transmitter:	
Frequency	52 MHz
Duty cycle	1 %
Peak power	72 kW (12 × 6 kW modules)
Pulse length	2 µs (300 m)
Pulse repetition	4096 Hz
Antenna:	12 × 12 array, 5-element Yagis
Spacing	0.71 λ
Area	44.4 m × 44.4 m
Receiver:	6 separate receivers
Sampling interval	2 µs (300 m)
Filter	half-width 500 kHz
Operation (ST-mode) time resolution:	1 min
http://www.irf.se/mst/EsrangeMST.html	

ACPD
11, 31475–31493, 2011

M. Mihalikova and S. Kirkwood

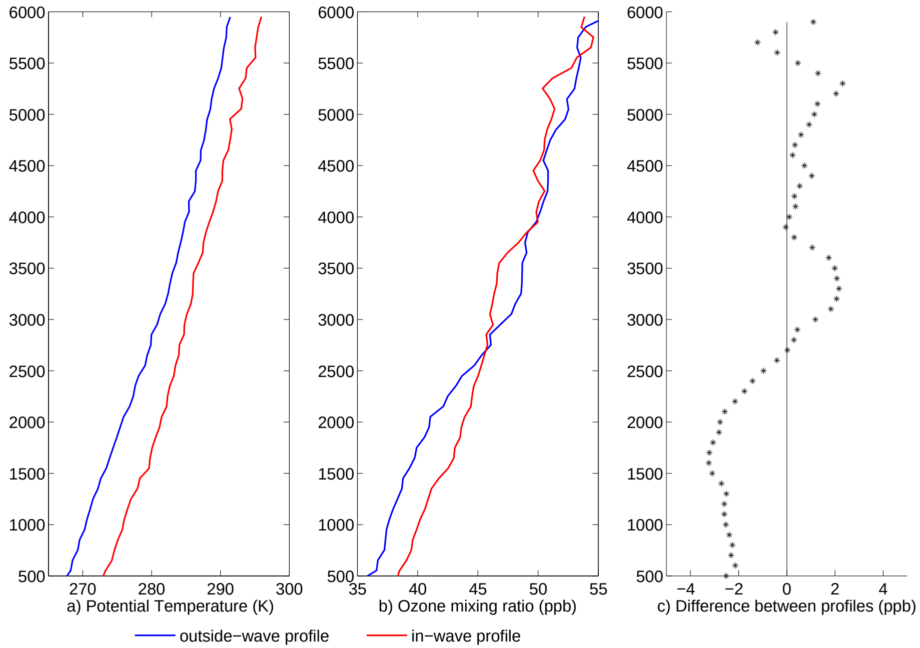

Fig. 1. Mean profiles of potential temperature **(a)**, ozone mixing ratio **(b)** and the difference between the profiles of ozone mixing ratio **(c)** for outside-wave (blue) and in-wave (red) group of ozonesondes.

ACPD
11, 31475–31493, 2011

Vertical mixing by mountain waves

M. Mihalikova and S. Kirkwood

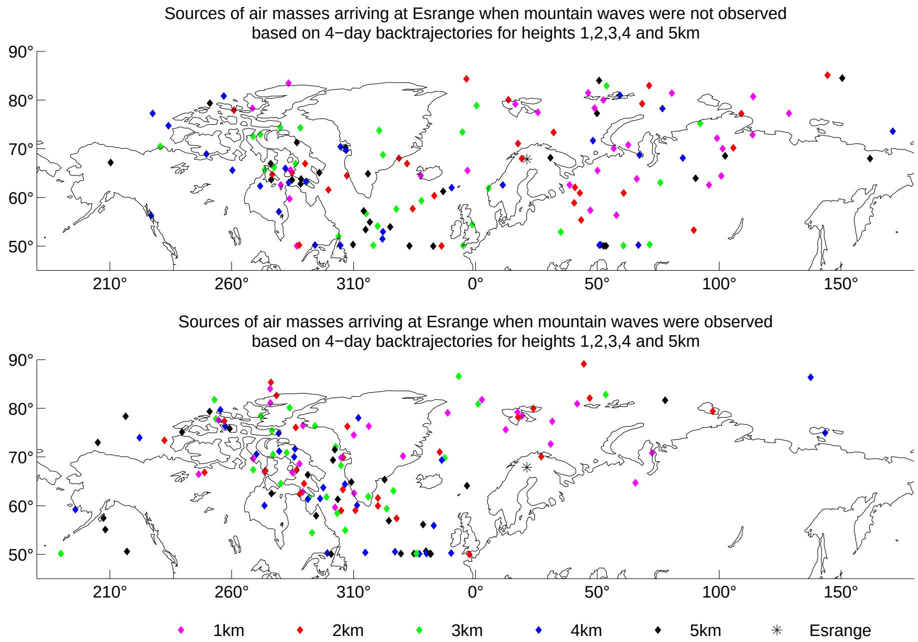

Fig. 2. Comparison, based on 4 d backtrajectories, of air mass sources between outside-wave (top) and in-wave (bottom) datasets when all sonde measurements were considered. Sources based on backtrajectories from individual heights 1, 2, 3, 4 and 5 km are displayed in various colors.

ACPD
11, 31475–31493, 2011

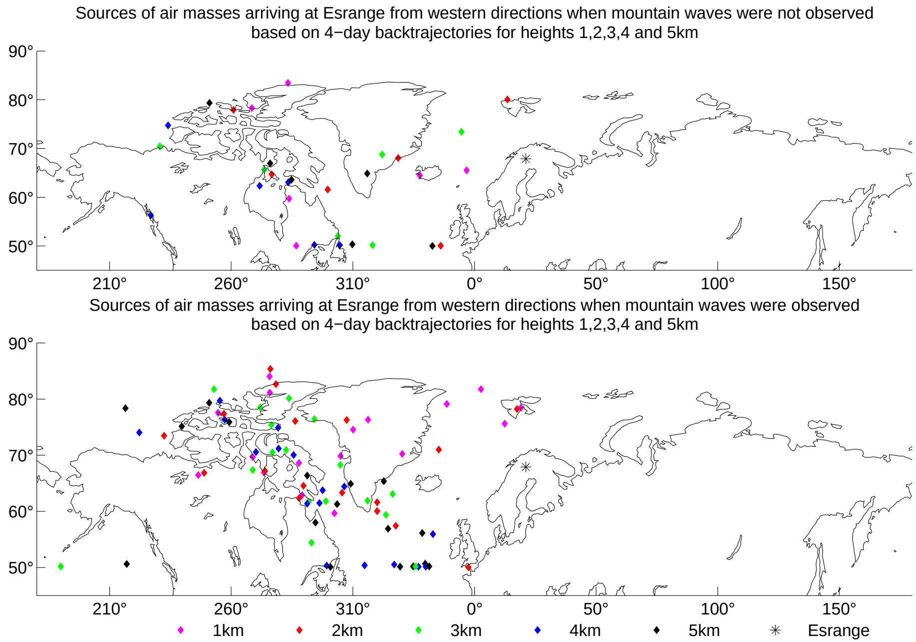

Fig. 3. Comparison, based on 4 d backtrajectories, of air mass sources between outside-wave (top) and in-wave (bottom) datasets after sondes with other than western sources in any of the heights were excluded. Sources based on backtrajectories from individual heights 1, 2, 3, 4 and 5 km are displayed in various colors.

ACPD
11, 31475–31493, 2011

M. Mihalikova and S. Kirkwood

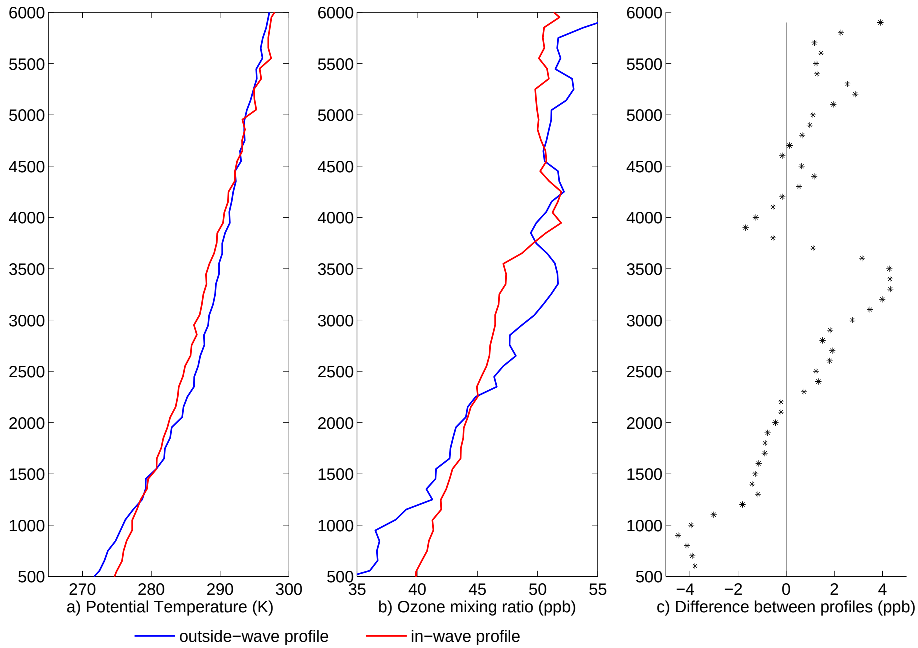

Fig. 4. Mean profiles of potential temperature **(a)**, ozone mixing ratio **(b)** and the difference between the profiles of ozone mixing ratio **(c)** for outside-wave (blue) and in-wave (red) group after limiting to sondes with western sources of air masses.